

Article

Garnets from the Sebadani metagabbro mass in the Sambagawa metamorphic belt, central Shikoku, Japan

Chihiro Enaka*, Akira Takasu* and Md. Fazle Kabir*

Abstract

The Sebadani area is located in the central part of the Besshi district; it is mainly composed of the eclogite-bearing Sebadani metagabbro mass and surrounding Seba basic schists (Seba eclogitic basic schists) with intercalation of pelitic and siliceous schists. Eclogites in the Sebadani metagabbro mass consist mainly of garnet, omphacite, amphibole (sodic, sodic-calcic and calcic) and epidote along with small amounts of rutile and titanite. Phengite, paragonite, albite, quartz and opaque minerals occur as accessories. Garnets exhibit two modes of occurrence and a wide range of chemical compositions suggesting a variety of equilibrium metamorphic $P-T$ conditions. Garnet 1 (Grt 1) occurs as porphyroblast and garnet 2 (Grt 2) is found as fine grain in the matrix. The texture of the minerals and their chemical compositions suggest the Seba metagabbro mass is characterized by two different metamorphic events according to the zoning of the garnets, i.e. a first high-pressure and high-temperature (HP-HT) metamorphic event and a second high-pressure metamorphic event. Garnet (Grt 1) is rich in almandine molecule and shows a prograde zoning. Chemical compositions of the fine grained garnet (Grt 2) are similar to the mantle to the rim of the porphyroblastic garnet (Grt 1). The outermost rim of the porphyroblastic garnet and fine-grained garnet shows another prograde growth zoning, and these outermost rims probably equilibrate in another eclogitic metamorphism.

Key words: Sambagawa metamorphic belt, Sebadani metagabbro mass, eclogite, garnet, omphacite

Introduction

The Sambagawa metamorphic belt is a high- P/T type metamorphic belt (Miyashiro, 1973) that stretches through southwest Japan over a length of approximately 800 km, from Saganoseki Peninsula in Kyushu to the Kanto Mountains in the northeast (Fig. 1). The dominant rock types within the belt consist of alternations of pelitic and basic schists, along with small amounts of siliceous and psammitic schists. Metamorphic conditions correspond to the pumpellyite-ac-tinolite, greenschist, blueschist and epidote-amphibolite facies (Banno, 1964; Higashino, 1990; Enami *et al.*, 1994). In the Besshi district, central Shikoku, the Sambagawa belt is divided into four zones based on the appearance of index minerals in pelitic schists, i.e. chlorite, garnet, albite-biotite and oligoclase-biotite zones (Enami, 1983; Higashino, 1990) (Fig. 1). Several coarse-grained eclogite-bearing ultramafic and mafic bodies occur within the albite-biotite and oligoclase-biotite zones, such as the the Higashi-akaishi peridotite mass, the Western Iratsu mass, and the Sebadani and the Tonaru metagabbro masses (e.g. Yokoyama, 1980; Takasu, 1984; Kunugiza *et al.*, 1986; Takasu, 1989; Aoya, 2001; Kugimiya and Takasu, 2002; Ota *et al.*, 2004; Miyagi and Takasu, 2005; Kabir and Takasu, 2010a, b; Endo and Tsuboi, 2013) (Fig. 1). These ultramafic-mafic masses underwent extensive recrystallization under epidote-amphibolite facies conditions. However, they locally preserve evidence of the

eclogite facies metamorphism (e.g. Takasu, 1989; Wallis and Aoya, 2000; Ota *et al.*, 2004; Kabir and Takasu, 2010a).

The Sebadani area is located in the central part of the Besshi district; it is mainly composed of the eclogite-bearing Sebadani metagabbro mass and surrounding Seba basic schists (Seba eclogitic basic schists) with intercalation of pelitic and siliceous schists (Figs. 1 and 2). Eclogites are sporadically preserved in the Seba eclogitic basic schists (Aoya, 2001; Zaw Win Ko *et al.*, 2005; Kabir and Takasu, 2010b). The Sebadani metagabbro mass was originally layered gabbro, and undergone eclogite facies metamorphism at higher temperature conditions than the surrounding Sebadani eclogitic basic schists (Takasu, 1984; Aoya, 2001; Kabir and Takasu, 2011).

In this paper we describe the diversity of texture and chemical compositions of the garnets from the Sebadani metagabbro mass. The mineral abbreviations used in the text, tables and figures follow Whitney and Evans (2010).

Petrography of the sebadani eclogites

Sebadani eclogites composed mainly of garnet, omphacite, amphibole (sodic, sodic-calcic and calcic) and epidote along with minor amounts of rutile and titanite. Phengite, paragonite, albite, quartz and opaque minerals occur as accessories. Eclogites are commonly massive, but they occasionally have a weak schistosity defined by preferred orientation of amphibole, epidote and omphacite.

The garnets in the eclogites are divided into two modes of occurrence. Grt 1 occurs as porphyroblast, and Grt 2

*Department of Geoscience, Graduate School of Science and Engineering, Shimane University, 1060 Nishikawatsu, Matsue 690-8504, Japan

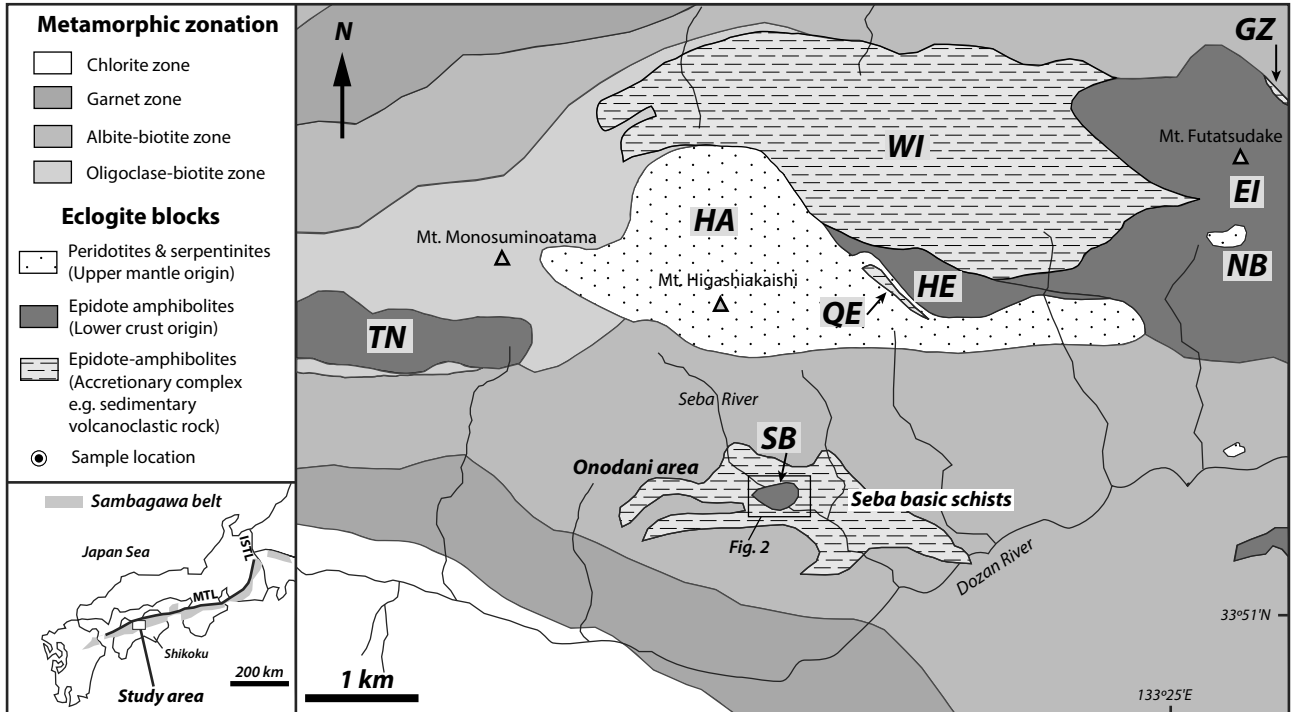


Fig. 1. Geological and metamorphic zonation map of the Sambagawa metamorphic belt in the Besshi district, central Shikoku, Japan (compiled from Takasu and Makino, 1980; Takasu, 1989; Higashino, 1990; Kugimiya and Takasu, 2002; Sakurai and Takasu, 2009; Kabir and Takasu, 2010a). SB, Seba metagabbro mass; TN, Tonaru metagabbro mass; WI, Western Iratsu mass; EI, Eastern Iratsu mass; HA, Higashi-akaishi peridotite mass; QE, Quartz eclogite mass; HE, Hornblende eclogite mass; NB, Nikubuchi peridotite mass; GZ, Gazo eclogite mass. The location of Fig. 2 is also showing.

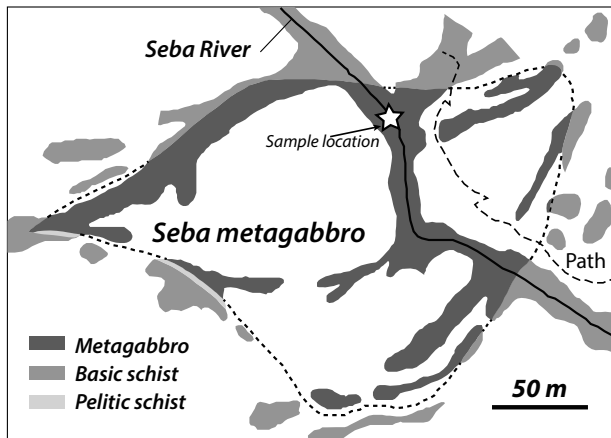


Fig. 2. Enlarged map of the Sebadani metagabbro after Aoya *et al.* (2006) and star indicated the location of collected sample for this study.

is found as fine grain in the matrix (Fig. 3). Grt1 occurs as euhedral to subhedral grain up to 1.5 mm across. It is optically zoned with pale orange core and almost colorless rim (Fig. 3a,c-d). The core of the garnet contains inclusions of omphacite, phengite, rutile and quartz. It also contains polyphase inclusions of phengite + quartz. Grt1 is intensely fractured, and the fractures are filled by omphacite, amphibole (glaucophane, barroisite, magnesiokatophorite), epidote, albite, rutile and titanite (Fig. 3a,g). Grt1 is sometimes replaced by amphibole (barroisite,

magnesiokatophorite) along the rim (Fig. 3c). Fine-grained garnets (Grt2) is euhedral to subhedral grain up to 0.6 mm across (Fig. 3b,e,f). It mostly lacks inclusions. It is optically zoned from pale orange core through colorless mantle to pale orange rim and the colorless outermost rim (Fig. 3e). Grt2 is sometimes fractured and the fractures are filled by amphibole (barroisite, magnesiokatophorite), rutile and quartz, and it is replaced by amphibole (barroisite, magnesiokatophorite) along the rim and the fracture (Fig. 3b).

Chemical compositions of the garnets

Chemical composition and compositional zoning of the garnets in the Sebadani metagabbro mass were investigated in Shimane University, using JEOL JXA 8800M and 8530F electron microprobe analyzers. Analytical conditions used for quantitative analysis were 15 kV accelerating voltage, 20 nA specimen current, and 5 μm beam diameter. Correction procedure was carried out as described by Bence and Albee (1968). Ferric iron contents in garnet were estimated using charge balance $\text{Fe}^{3+}=8-2\text{Si}-2\text{Ti}-\text{Al}$ ($\text{O}=12$). Na (<0.22 wt%), K (<0.10 wt%) and Cr (<0.13 wt%) contents in the garnets are negligible.

In the Sebadani metagabbro mass, porphyroblastic garnet (Grt1) has almandine and grossular-rich in composition (X_{Alm} 0.39-0.55, X_{Grs} 0.29-0.34) with variable amounts of pyrope (X_{Pyr} 0.18-0.30) and spessartine (X_{SpS} 0-0.04) (Fig. 4a-d). Garnet (Grt1) shows a compositional zoning with decreas-

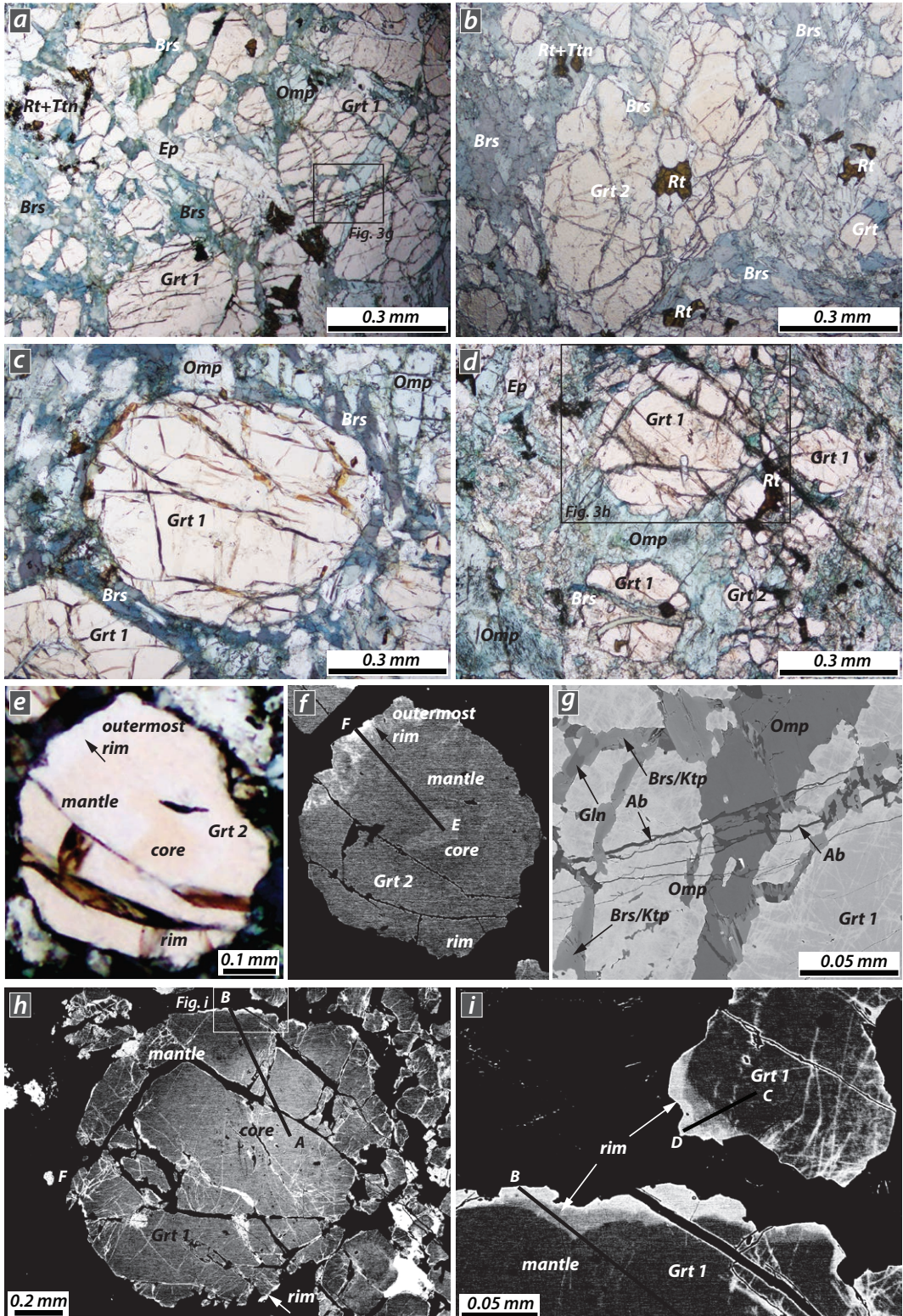


Fig 3. Photomicrographs and backscattered electron images (BEI) of eclogites in the Sebadani metagabbro mass.
 (a) Porphyroblastic garnet (Grt 1) is fractured and the fractures are filled by omphacite, barroisite and epidote. (b) Fine-grained garnet in the matrix contains inclusions of rutile. Barroisite in garnet fracture-filling and other matrix minerals of barroisite, rutile and titanites are also shown. (c) Porphyroblastic garnet and coexisting omphacite in the matrix. Garnet (Grt 1) partly replaced by barroisitic amphibole. (d) Porphyroblastic garnet (Grt 1), fine grained garnet (Grt2) and coexisting omphacite, epidote and rutile in the matrix. (e) Photomicrograph of a fine-grained garnet and BEI of the same garnet (f). (g) Fractures in the porphyroblastic garnet (Grt 1) are filled by omphacite, amphibole (Brs, Ktp), Gln and albite. Location of this figure is shown in Fig. 3a. (h) BEI of porohyroblastic garnet (Grt 1) shown in Fig. 3d showing a zoning with light core, relatively dark mantle and light rim. (i) Dark colored rim and gray to light gray outermost rim of the porphyroblastic garnet (Grt 1).

ing and increasing X_{Prp} (0.21-0.15-0.20), antithetic zoning of X_{Alm} (0.49-0.51-0.45) and increasing X_{Grs} (0.28-0.32) and homogeneous X_{Sps} (0.03) from inner core to outer core. Inner mantle to outer mantle of the garnet shows increasing X_{Alm} (0.45-0.50), increasing and decreasing X_{Prp} (0.20-0.24-0.17), decreasing X_{Sps} (0.03-0.01) and homogeneous X_{Grs} (0.32). Rim of the garnet shows further increasing and at the outermost rim slight decreasing in pyrope (X_{Prp} 0.17-0.19-0.15) and antithetic zoning of spessartine (X_{Sps} 0.02-0.01-0.03), sharply increasing in almandine (X_{Alm} 0.45-0.55) and decreasing grossular (X_{Grs} 0.32-0.27) (Fig. 4a, c-d). Some other porphyroblastic garnet (Grt 1) rim also shows similar zoning with increasing and slight decreasing of X_{Prp} (0.17-0.18-0.13) and decreasing and increasing of spessartine (X_{Sps} 0.02-0.01-0.04) from inner part towards outer most rim (Fig. 4b).

Fine-grained garnet (Grt 2) also shows almandine and grossular-rich in composition (X_{Alm} 0.41-0.59, X_{Grs} 0.24-0.32) with variable amounts of pyrope (0.13-0.31) and spessartine (X_{Sps} 0-0.04) (Fig. 4e-h). The core of the fine-grained garnets (Grt 2) shows slight increasing in pyrope (X_{Prp} 0.26-0.28), decreasing in almandine (X_{Alm} 0.44-0.42) and grossular (X_{Grs} 0.30-0.28), spessartine (X_{Sps} 0.01-0.01) compositions are homogeneous (Fig. 4e-g). The mantle of the garnet is characterized by a zoning showing increasing pyrope (X_{Prp} 0.26-0.27) and almandine (X_{Alm} 0.42-0.44), and decreasing grossular (X_{Grs} 0.29-0.28) and homogeneous in spessartine compositions (X_{Sps} 0.01-0.01) (Fig. 4e-g). The rim of these garnet shows increasing in pyrope (X_{Prp} 0.24-0.27) and grossular (X_{Grs} 0.28-0.32) and decreasing almandine (X_{Alm} 0.44-0.42) and homogeneous in spessartine (X_{Sps} 0.01-0) compositions (Fig. 4e-g). Chemical compositions of the fine-grained garnet (Grt 2) are similar to mantle to rim of the porphyroblastic garnet (Grt 1). The colorless outermost rim of the fine-grained garnet (Grt 2) shows slight increasing and rapid decreasing and farther increasing pyrope (X_{Prp} 0.27-0.30-0.13-0.17) and antithetic zoning of almandine (X_{Alm} 0.45-0.44-0.59-0.56) and spessartine (X_{Sps} 0.01-0-0.04-0.03) from inner part towards the outermost rim (Fig. 4e,h).

Discussion and Conclusions

Two modes of occurrence and wide range of chemical compositions of the garnets in the Seba metagabbro mass suggest a variety of equilibrium metamorphic P - T conditions.

Takasu (1984) reported that the garnets within the eclogites in the Sebadani metagabbro mass contain two zones, core and rim. The core is richer in pyrope (X_{Prp} 0.13-0.29) and poorer in almandine (X_{Alm} 0.43-0.57) and spessartine (X_{Sps} 0.01-0.03) than the rim (X_{Prp} 0.13-0.15; X_{Alm} 0.55-0.61; X_{Sps} 0.01-0.05) (Fig. 4c and h). The core of the garnets undergone eclogite facies metamorphism at higher temperature conditions ($821 \pm 32^\circ\text{C}$ and 19.4 ± 1.6 kbar) than the surrounding Sebadani eclogitic basic schists (Takasu, 1984; Kabir and Takasu, 2011). The rim of the garnets also suffered an eclogitic metamorphism and this event

probably correlated with the eclogite facies metamorphism of the surrounding Seba eclogitic basic schists (610 - 640°C and 12-24 kbar) (Aoya, 2001).

The textures of the minerals and chemical compositions suggest the Sebadani metagabbro mass is characterized by two different metamorphic events, and they are represented by the zoning of the garnets, i.e. a first high-pressure and high-temperature (HP-HT) metamorphic event and a second high-pressure metamorphic event. Garnet (Grt 1) is rich in almandine contents and shows a prograde growth zoning. The mineral assemblages of the inclusions in the cores (omphacite, phengite, rutile and quartz) of the garnets suggest a prograde path of high- T eclogitic metamorphism during the first HP-HT metamorphic event. Chemical compositions of the fine grained garnet (Grt 2) are similar to mantle to rim of the porphyroblastic garnet (Grt 1) probably shared similar metamorphic history.

The colorless outermost rim of the fine grained garnet (Grt 2) shows rapid decrease and farther increase in pyrope (X_{Prp} 0.30-0.13-0.17) and antithetic zoning of almandine (X_{Alm} 0.44-0.59-0.56) and spessartine (X_{Sps} 0-0.04-0.03) from inner part towards the outermost rim (Fig. 4e). The rim of the garnet (Grt 1) also shows a similar zoning with an increase and slight decrease at the outermost rim in pyrope (X_{Prp} 0.17-0.19-0.15) and antithetic zoning of spessartine (X_{Sps} 0.02-0.01-0.03) contents (Fig. 4a). The rim of the porphyroblastic garnet (Grt 1) and outermost rim of Grt 2 shows another prograde growth zoning. The rim (Grt 1) and the outermost rim (Grt 2) are probably equilibrated in another eclogitic metamorphism. The chemical compositions of the porphyroblastic (Grt 1) and fine-grained garnet (Grt 2) are similar to those of the pyrope-rich core and rim of the Grt 1 garnet and outermost rim of fine-grained garnet (Grt 2) are similar to those of rim of the Sebadani metagabbro mass by Takasu (1984). The porphyroblastic garnet (Grt 1) in this study suffered a prograde metamorphism and probably follow a similar peak metamorphism of the Sebadani metagabbro mass by Takasu (1984). Rims of the porphyroblastic garnet (Grt 1) and outermost rim of fine-grained garnet (Grt 2) probably follow a similar prograde and peak metamorphism of the surrounding Seba eclogitic basic schists by Aoya (2001).

Acknowledgements

We thank the members of the Metamorphic Geology Seminar of Shimane University for their discussion and helpful suggestions, and Hiroaki Komuro for critical reading and comments on the manuscript. Thanks are also due to Yasunori Kondo for his support during fieldwork. This study was partly supported by JSPS KAKENHI Grant (No. 24340123) to A.T.

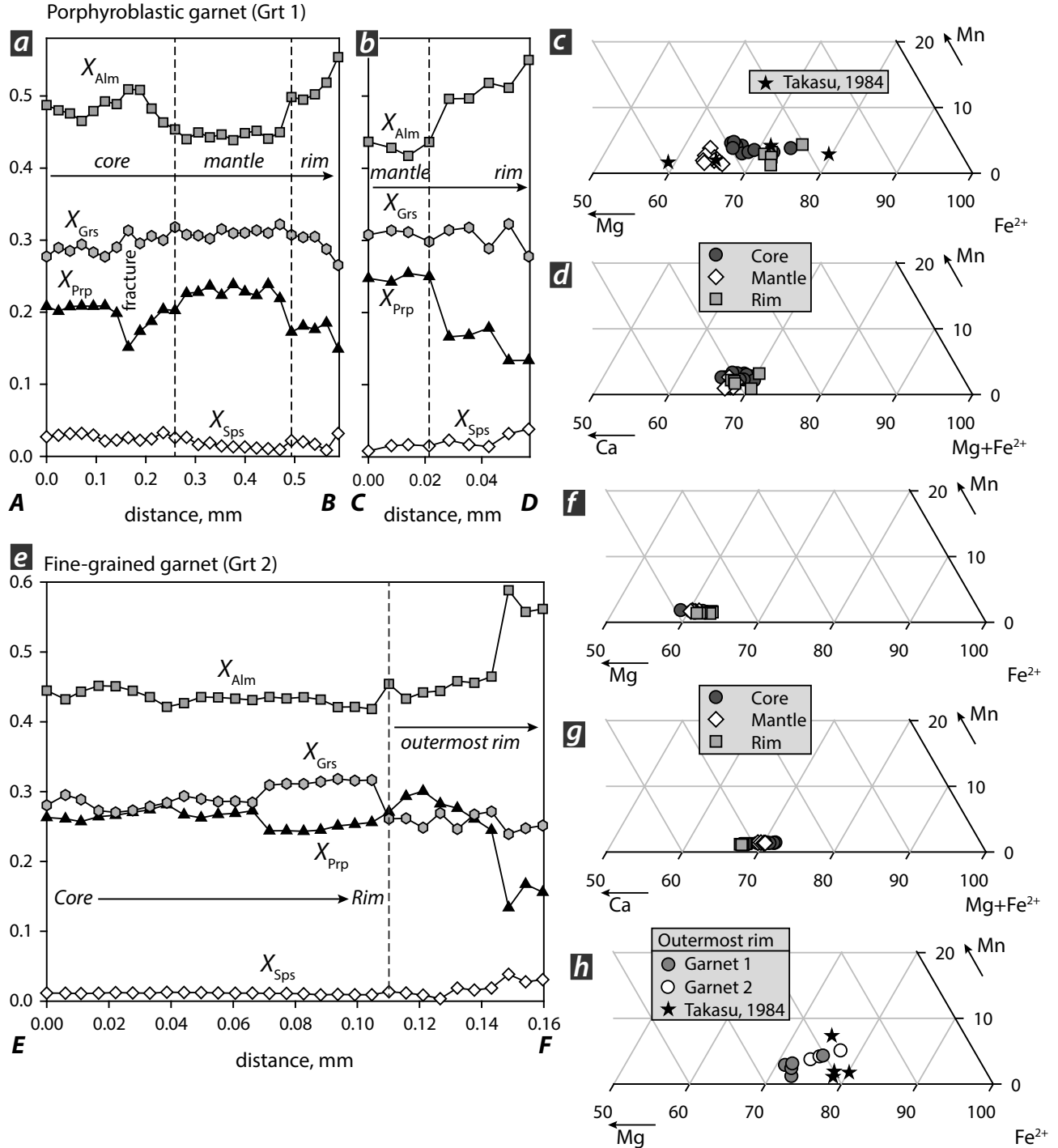


Fig. 4. Chemical compositions of zoned garnets from the Sebadani metagabbro mass. (a) Compositional profile of porphyroblastic garnet (Grt 1) from core to rim in terms of X_{Alm} , X_{Prp} , X_{Grs} and X_{Spes} (from Fig. 3h). (b) Compositional profile of mantle and rim of the garnet (Grt 1) (from figure 3i). (c) composition of garnet (Grt 1) in terms of Fe^{2+} , Mn and Mg and compositions of pyrope-rich garnets by Takasu (1984) are also showing. (d) Composition of garnet (Grt 1) in terms of $\text{Mg} + \text{Fe}^{2+}$, Mn and Ca . (e) Core through rim to the outermost rim of compositional profile of fine-grained garnet (Grt 2) in terms of X_{Alm} , X_{Prp} , X_{Grs} and X_{Spes} (from Fig. 3f). (f) chemical composition of garnet (Grt 2) in terms of Fe^{2+} , Mn and Mg and in terms of $\text{Mg} + \text{Fe}^{2+}$, Mn and Ca (g). (h) Chemical compositions of the rim (Grt 1) and outermost rim (Grt 2) of the garnet and almandine-rich garnets from the Sebadani metagabbro mass by Takasu (1984) are also shown.

References

- Aoya, M., 2001, *P-T-D* path of eclogite from the Sambagawa belt deduced from combination of petrological and microstructural analyses. *Journal of Petrology*, **42**, 1225-1248.
- Aoya, M., Tsuboi, M. and Wallis, S. R., 2006, Origin of eclogitic metagabbro mass in the Sambagawa belt: Geological and geochemical constraints. *Lithos*, **89**, 107-134.
- Banno, S., 1964, Petrological studies of the Sanbagawa crystalline schists in the Besshi-Ino district, central Shikoku, Japan. *Journal of the Faculty of Science, Tokyo University, Section II*, **15**, 203-319.
- Bence, A. E. and Albee, A. L., 1968, Empirical correction factors for the electron microanalysis of silicates and oxides. *Journal of Geology*, **76**, 382-403.
- Enami, M., 1983, Petrology of pelitic schists in the oligoclase-biotite zone of the Sanbagawa metamorphic terrain, Japan: phase equilibria in the highest grade zone of a high-pressure intermediate type of metamorphic belt. *Journal of Metamorphic Geology*, **1**, 141-161.
- Enami, M., Wallis, S. R. and Banno, Y., 1994, Paragenesis of sodic pyroxene-bearing quartz schists: implications for the *P-T* history of the Sanbagawa belt. *Contributions to Mineralogy and Petrology*, **116**, 182-198.
- Endo, S. and Tsuboi, M., 2013, Petrogenesis and implications of jadeite-bearing kyanite eclogite from the Sanbagawa belt (SW Japan). *Journal of Metamorphic Geology*, **31**, 647-661.
- Higashino, T., 1990, The higher grade metamorphic zonation of the Sanbagawa metamorphic belt in central Shikoku, Japan. *Journal of Metamorphic Geology*, **8**, 413-423.
- Kabir, M. F. and Takasu, A., 2010a, Evidence for multiple burial-partial exhumation cycles from the Onodani eclogites in the Sanbagawa metamorphic belt, central Shikoku, Japan. *Journal of Metamorphic Geology*, **28**, 873-893.
- Kabir, M. F. and Takasu, A., 2010b, Glaucophanic amphibole in the Seba eclogitic basic schists, Sanbagawa metamorphic belt, central Shikoku, Japan: implications for timing of juxtaposition of the eclogite body with the non-eclogite Sanbagawa schists. *Earth Sciences*, **64**, 183-192.
- Kabir, M. F. and Takasu, A., 2011, High-Mg garnets from pelitic schists adjacent to the Sebadani eclogitic metagabbro mass, Sanbagawa metamorphic belt, central Shikoku, Japan. *Journal of Mineralogical and Petrological Sciences*, **106**, 332-337.
- Kugimiya, Y. and Takasu, A., 2002, Geology of the Western Iratsu mass within the tectonic melange zone in the Sanbagawa metamorphic belt, Besshi district, central Shikoku, Japan. *Journal of the Geological Society of Japan*, **108**, 644-662.
- Kunugiza, K., Takasu, A. and Banno, S., 1986, The origin and metamorphic history of the ultramafic and metagabbro bodies in the Sanbagawa Metamorphic Belt. *Geological Society of America Memoir*, **164**, 375-386.
- Miyagi, Y. and Takasu, A., 2005, Prograde eclogites from the Tonaru epidote amphibolite mass in the Sanbagawa Metamorphic Belt, central Shikoku, southwest Japan. *Island Arc*, **14**, 215-235.
- Miyashiro, A., 1973, *Metamorphism and metamorphic belts*. George Allen and Unwin, London, England.
- Ota, T., Terabayashi, M. and Katayama, I., 2004, Thermobaric structure and metamorphic evolution of the Iratsu eclogite body in the Sanbagawa belt, central Shikoku, Japan. *Lithos*, **73**, 95-126.
- Sakurai, T. and Takasu, A., 2009, Geology and metamorphism of the Gazo mass (eclogite-bearing tectonic block) in the Sanbagawa metamorphic belt, Besshi district, central Shikoku, Japan. *Journal of Geological Society of Japan*, **115**, 101-121.
- Takasu, A., 1984, Prograde and retrograde eclogites in the Sanbagawa metamorphic belt, Besshi district, Japan. *Journal of Petrology*, **25**, 619-643.
- Takasu, A., 1989, *P-T* histories of peridotite and amphibolite tectonic blocks in the Sanbagawa metamorphic belt, Japan. In: *Evolution of Metamorphic Belts* (eds Daly, J. S., Cliff, R. A. & Yardley, B. W. D.), Geological Society, London, Special Publications, **43**, 533-538, Blackwell Scientific Publications, Oxford.
- Takasu, A. and Makino, K., 1980, Stratigraphy and geologic structure of the Sanbagawa metamorphic belt in the Besshi district, Shikoku, Japan (Reexamination of the recumbent fold structures). *Earth Science*, **34**, 16-26 (in Japanese with English abstract).
- Wallis, S. R. and Aoya, M., 2000, A re-evaluation of eclogite facies metamorphism in SW Japan: proposal for an eclogite nappe. *Journal of Metamorphic Geology*, **18**, 653-664.
- Whitney, D. L. and Evans, B. W., 2010, Abbreviations for names of rock-forming minerals. *American Mineralogist*, **95**, 185-187.
- Yokoyama, K., 1980, Nikubuchi peridotite body in the Sanbagawa metamorphic belt; thermal history of the 'Al-pyroxene-rich suite' peridotite body in high pressure metamorphic terrain. *Contributions to Mineralogy and Petrology*, **73**, 1-13.
- Zaw Win Ko, Enami, M. and Aoya, M., 2005, Chloritoid and barroisite-bearing pelitic schists from the eclogite unit in the Besshi district, Sanbagawa metamorphic belt. *Lithos*, **81**, 79-100.

(Received: Nov. 26, 2014, Accepted: Jan. 19, 2015)

(要旨)

江中千簡・高須 晃・Kabir, Md. Fazle, 2014 四国中央部三波川変成帯瀬場谷変斑れい岩中のざくろ石島根大学地球資源環境学研究報告, **33**, 19-27.

四国中央部別子地域の中心部に位置する瀬場谷地域は、エクロジヤイトを伴う瀬場谷変斑れい岩体とその周囲に瀬場塩基性片岩（エクロジヤイト質塩基性片岩）が分布する。瀬場谷変斑れい岩体のエクロジヤイトは、主成分鉱物としてざくろ石、オンファス輝石、角閃石（Na, Na-Ca, Ca 角閃石）、緑れん石、副成分鉱物としてルチル、チタン石、微量成分鉱物としてフェンジヤイト、パラゴナイト、曹長石、石英、不透明鉱物を含む。ざくろ石には2つの産状（ざくろ石1とざくろ石2）がある。ざくろ石1は斑状変晶、ざくろ石2は基質中において細粒結晶として産する。ざくろ石の組織と化学組成により、瀬場谷変斑れい岩体が2度の異なる変成イベント（第1高温-高压変成イベント、第2高压変成イベント）によって特徴づけられることを示す。ざくろ石1はアルマンディン成分に富み、昇温の累帶構造を示す。ざくろ石2の化学組成は、ざくろ石1のマントルからリムと似ている。ざくろ石1とざくろ石2のリム最外縁部は、別の昇温期の成長を示し、これらのリム最外縁部は、異なるエクロジヤイト相変成作用において成長した可能性を示す。

Table 1. Representative chemical compositions of garnets from the Sebadani metagabbro mass.

Sample	ES 20-1																			
	23	24	25	26	27	28	29	30	31	32	33	34	35	36	37	38	39	40	41	
Analysis	Grt 1	Grt 1	Grt 1	Grt 1	Grt 1	Grt 1	Grt 1	Grt 1	Grt 1	Grt 1	Grt 1	Grt 1	Grt 1	Grt 1	Grt 1	Grt 1	Grt 1	Grt 1	Grt 1	Grt 1
Mode																				
Core	→	→	→	→	→	→	→	→	→	→	→	→	→	→	→	→	→	→	→	→
SiO ₂	38.18	38.47	38.51	38.38	39.08	38.22	38.41	38.54	38.61	39.66	38.78	38.36	38.44	39.11	38.47	39.41	39.17	39.14	39.37	
TiO ₂	0.10	0.25	0.02	0.03	0.07	0.15	0.00	0.07	0.04	0.12	0.00	0.09	0.00	0.10	0.05	0.10	0.04	0.11	0.07	
Al ₂ O ₃	20.60	20.75	21.27	20.78	21.38	20.26	21.11	21.06	20.53	20.67	21.57	21.34	21.24	20.98	21.10	21.73	20.89	20.96	21.32	
FeO*	23.02	23.20	22.52	23.11	22.72	23.34	23.45	22.62	22.78	21.69	21.19	23.05	21.59	21.37	21.28	20.94	20.84	21.52	20.67	
MnO	1.94	1.88	1.66	1.62	1.44	1.47	1.31	1.17	0.82	0.98	0.46	0.63	0.66	0.46	0.46	0.40	0.13	0.00	0.26	
MgO	5.55	4.99	5.00	5.43	4.72	5.03	5.49	4.94	5.15	5.69	5.51	5.30	5.73	5.58	5.83	6.44	6.69	7.23	7.01	
CaO	10.78	10.52	10.85	10.44	10.32	11.17	10.78	10.81	11.58	11.49	11.83	12.10	11.54	11.96	11.90	11.24	12.13	11.22	11.05	
Total	100.17	100.06	99.83	99.79	99.73	99.64	100.55	99.21	99.51	100.30	99.34	100.87	99.20	99.56	99.09	100.26	99.89	100.18	99.75	
<i>Cations on the basis of 12 oxygens</i>																				
Si	2.96	2.99	2.99	2.99	3.05	2.98	2.96	3.01	3.05	3.00	2.94	2.99	3.03	2.99	3.01	3.00	2.99	3.02		
Ti	0.01	0.02	0.00	0.00	0.01	0.00	0.00	0.00	0.01	0.00	0.01	0.00	0.01	0.00	0.01	0.00	0.01	0.00	0.00	
Al	1.88	1.90	1.95	1.90	1.96	1.87	1.92	1.94	1.89	1.88	1.97	1.93	1.95	1.91	1.93	1.96	1.89	1.89	1.93	
Fe ³⁺	0.19	0.08	0.06	0.12	0.00	0.15	0.16	0.02	0.09	0.00	0.02	0.17	0.08	0.02	0.09	0.00	0.10	0.12	0.03	
Fe ²⁺	1.30	1.43	1.41	1.38	1.48	1.38	1.35	1.46	1.39	1.40	1.36	1.31	1.32	1.37	1.30	1.34	1.24	1.25	1.29	
Mn	0.13	0.12	0.11	0.11	0.10	0.10	0.09	0.08	0.05	0.06	0.03	0.04	0.04	0.03	0.03	0.03	0.01	0.00	0.02	
Mg	0.64	0.58	0.58	0.63	0.55	0.58	0.63	0.58	0.60	0.65	0.64	0.61	0.66	0.64	0.67	0.73	0.76	0.82	0.80	
Ca	0.89	0.88	0.90	0.87	0.86	0.93	0.89	0.91	0.97	0.95	0.98	0.99	0.96	0.99	0.92	1.00	0.92	0.91	0.91	
Total	8.00	8.00	8.00	8.00	8.00	8.00	8.00	8.00	8.00	8.00	8.00	8.00	8.00	8.00	8.00	8.00	8.00	8.00	8.00	
<i>X_{Prp}</i>																				
<i>X_{alm}</i>	0.22	0.19	0.19	0.21	0.18	0.20	0.21	0.19	0.20	0.21	0.21	0.21	0.22	0.21	0.23	0.24	0.26	0.27	0.26	
<i>X_{Grs}</i>	0.44	0.48	0.47	0.46	0.50	0.46	0.46	0.48	0.46	0.46	0.45	0.44	0.44	0.45	0.43	0.44	0.41	0.42	0.43	
<i>X_{Sp}</i>	0.30	0.29	0.30	0.29	0.29	0.31	0.30	0.30	0.32	0.31	0.33	0.34	0.32	0.33	0.33	0.31	0.33	0.31	0.30	
<i>X_{Sp}</i>	0.04	0.04	0.04	0.03	0.03	0.03	0.03	0.02	0.02	0.01	0.01	0.01	0.02	0.01	0.01	0.01	0.01	0.00	0.01	

*Total Fe as FeO

Sample	ES 20-1																			
	42	43	44	45	46	47	48	49	50	51	52	53	54	55	56	1	2	3	4	
Analysis	Grt 1	Grt 1	Grt 1	Grt 1	Grt 1	Grt 2	Grt 2	Grt 2	Grt 2	Grt 2	Grt 2	Grt 2	Grt 2	Grt 2	Grt 2	Grt 2	Grt 2	Grt 2	Grt 2	
Mode						→	→	Rim	Rim	↔	↔	↔	↔	↔	↔	↔	↔	↔	↔	
Core	→	→	→	→	→	→	→	→	→	→	→	→	→	→	→	→	→	→	→	
SiO ₂	39.76	39.75	38.47	39.50	38.84	39.14	38.09	38.62	38.97	38.62	38.50	38.29	38.43	38.57	38.66	39.39	39.60	39.40	39.78	
TiO ₂	0.00	0.01	0.00	0.19	0.14	0.03	0.05	0.00	0.00	0.02	0.00	0.00	0.04	0.13	0.07	0.06	0.00	0.10	0.05	
Al ₂ O ₃	21.85	21.75	21.29	21.25	21.03	22.18	21.03	21.16	22.30	21.71	21.64	21.40	21.41	21.92	21.18	21.67	22.01	21.44	21.80	
FeO*	20.76	19.55	20.73	20.83	20.88	21.86	22.68	22.70	21.72	22.43	23.16	22.89	27.09	25.07	25.65	20.01	19.58	20.02	19.19	
MnO	0.53	0.40	0.30	0.30	0.59	0.62	0.52	0.39	0.16	0.85	0.72	0.85	1.74	1.23	1.39	0.46	0.68	0.20	0.39	
MgO	6.99	6.55	7.63	6.80	6.82	6.58	6.70	6.91	7.38	7.10	6.72	6.29	3.45	4.22	4.00	7.58	6.84	7.38	6.97	
CaO	10.70	11.49	10.95	10.81	10.99	9.55	9.27	8.90	9.78	8.81	9.58	9.71	8.57	8.69	8.96	10.96	11.70	11.48	11.71	
Total	100.59	99.50	99.37	99.58	99.41	100.50	99.11	99.52	100.31	99.54	100.32	99.43	100.73	99.83	99.91	100.13	100.41	100.02	99.89	
<i>Cations on the basis of 12 oxygens</i>																				
Si	3.03	3.05	2.95	3.04	2.99	2.98	2.95	2.97	2.98	2.95	2.97	2.97	3.01	3.02	3.04	3.00	3.01	3.00	3.04	
Ti	0.00	0.00	0.00	0.01	0.01	0.00	0.00	0.00	0.00	0.00	0.00	0.00	0.00	0.00	0.00	0.00	0.00	0.00	0.00	
Al	1.96	1.97	1.93	1.93	1.91	1.99	1.92	1.92	2.00	1.97	1.96	1.95	1.98	2.03	1.96	1.94	1.97	1.93	1.96	
Fe ³⁺	0.00	0.00	0.00	0.17	0.00	0.09	0.04	0.18	0.14	0.06	0.07	0.13	0.10	0.00	0.00	0.06	0.01	0.06	0.00	
Fe ²⁺	1.32	1.26	1.16	1.34	1.26	1.36	1.29	1.32	1.32	1.38	1.35	1.38	1.77	1.64	1.69	1.22	1.24	1.22	1.22	
Mn	0.03	0.03	0.02	0.02	0.04	0.04	0.03	0.03	0.01	0.05	0.05	0.06	0.12	0.08	0.09	0.03	0.04	0.01	0.03	
Mg	0.79	0.75	0.87	0.77	0.79	0.81	0.86	0.89	0.84	0.82	0.77	0.73	0.40	0.49	0.47	0.86	0.78	0.84	0.79	
Ca	0.87	0.94	0.90	0.89	0.91	0.78	0.77	0.80	0.80	0.79	0.81	0.72	0.73	0.75	0.89	0.95	0.94	0.96	0.96	
Total	8.00	8.00	8.00	8.00	8.00	8.00	8.00	8.00	8.00	8.00	8.00	8.00	8.00	8.00	8.00	8.00	8.00	8.00	8.00	
<i>X_{Prp}</i>																				
<i>X_{alm}</i>	0.26	0.25	0.30	0.25	0.27	0.29	0.30	0.28	0.28	0.26	0.25	0.25	0.13	0.16	0.16	0.29	0.26	0.28	0.26	
<i>X_{Grs}</i>	0.44	0.42	0.39	0.44	0.42	0.46	0.44	0.45	0.46	0.46										

Table 1. (continued)

Sample		ES 20-1																			
		Grt 2																			
Analysis		52	53	54	55	56	57	58	59	60	61	62	63	64	65	66	67	68	69	70	
Mode		Grt 2	Grt 2	Grt 2	Grt 2	Grt 2	Grt 2	Grt 2	Grt 2	Grt 2	Grt 2	Grt 2	Grt 2	Grt 2	Grt 2	Grt 2	Grt 2	Grt 2	Grt 2	Grt 2	
		→	→	→	→	→	→	→	→	→	Rim	Rim	→	→	→	→	→	Rim	Rim	→	
SiO ₂		39.97	40.13	40.51	40.14	39.72	40.00	40.04	39.93	40.17	39.89	40.05	39.77	39.85	39.70	39.96	39.60	39.57	39.74	40.12	
TiO ₂		0.02	0.01	0.02	0.00	0.07	0.03	0.04	0.04	0.04	0.02	0.00	0.04	0.00	0.00	0.01	0.02	0.04	0.01	0.01	
Al ₂ O ₃		22.17	22.26	22.44	22.08	21.88	22.04	22.14	21.94	22.35	22.00	22.10	21.96	22.05	22.11	21.99	21.77	21.81	22.02	22.02	
FeO*		21.09	20.59	20.40	20.20	20.93	20.75	21.05	22.34	21.53	22.14	20.04	20.98	20.78	21.55	22.02	24.07	24.57	20.62	20.50	
MnO		0.47	0.39	0.35	0.40	0.37	0.44	0.51	0.68	0.69	0.78	0.43	0.56	0.51	0.63	0.67	1.01	1.56	0.42	0.43	
MgO		6.71	7.39	7.41	7.54	7.19	7.15	6.85	5.99	6.00	5.64	6.99	6.63	6.90	5.81	5.63	4.39	3.50	6.72	6.73	
CaO		9.59	9.27	9.37	9.44	9.05	9.05	9.26	9.59	9.87	9.71	9.72	9.44	9.30	9.20	9.16	9.00	8.94	10.02	9.45	
Total		100.02	100.04	100.50	99.80	99.21	99.46	99.88	100.51	100.65	100.20	99.35	99.34	99.43	99.00	99.43	99.85	99.97	99.58	99.26	
<i>Cations on the basis of 12 oxygens</i>																					
Si		3.06	3.06	3.08	3.06	3.06	3.07	3.07	3.06	3.07	3.08	3.07	3.07	3.09	3.10	3.09	3.11	3.05	3.10		
Ti		0.00	0.00	0.00	0.00	0.00	0.00	0.00	0.00	0.00	0.00	0.00	0.00	0.00	0.00	0.00	0.00	0.00	0.00	0.00	
Al		2.00	2.00	2.01	1.99	1.99	2.00	2.00	1.98	2.01	2.00	2.00	2.00	2.03	2.01	2.01	2.02	1.99	2.00		
Fe ³⁺		0.00	0.00	0.00	0.00	0.00	0.00	0.00	0.00	0.00	0.00	0.00	0.00	0.00	0.00	0.00	0.00	0.00	0.00	0.00	
Fe ²⁺		1.35	1.31	1.29	1.29	1.35	1.33	1.35	1.43	1.38	1.43	1.29	1.35	1.34	1.40	1.43	1.57	1.61	1.33	1.32	
Mn		0.03	0.03	0.02	0.03	0.02	0.03	0.05	0.05	0.05	0.03	0.04	0.03	0.04	0.05	0.07	0.10	0.03	0.03	0.03	
Mg		0.77	0.84	0.84	0.86	0.83	0.82	0.79	0.69	0.68	0.65	0.80	0.76	0.79	0.67	0.65	0.51	0.41	0.77	0.77	
Ca		0.79	0.76	0.76	0.75	0.75	0.76	0.79	0.81	0.80	0.80	0.78	0.77	0.76	0.75	0.75	0.83	0.78			
Total		8.00	8.00	8.00	8.00	8.00	8.00	8.00	8.00	8.00	8.00	8.00	8.00	8.00	8.00	8.00	8.00	8.00	8.00	8.00	
X _{Pp}		0.26	0.29	0.29	0.29	0.28	0.28	0.27	0.23	0.22	0.22	0.28	0.26	0.27	0.23	0.22	0.18	0.14	0.26	0.27	
X _{alm}		0.46	0.45	0.44	0.44	0.46	0.46	0.46	0.49	0.47	0.49	0.44	0.46	0.46	0.49	0.50	0.54	0.56	0.45	0.45	
X _{Grs}		0.27	0.26	0.26	0.26	0.25	0.25	0.26	0.27	0.28	0.27	0.27	0.27	0.26	0.27	0.26	0.26	0.28	0.27	0.27	
X _{Sps}		0.01	0.01	0.01	0.01	0.01	0.01	0.01	0.02	0.02	0.01	0.01	0.01	0.01	0.01	0.01	0.02	0.02	0.04	0.01	

*Total Fe as FeO

Sample		ES 20-1																			
		Grt 2																			
Analysis		71	72	73	74	75	76	77	78	79	80	81	82	83	84	85	86	87	88	89	
Mode		Grt 2	Grt 2	Grt 2	Grt 2	Grt 2	Grt 2	Grt 2	Grt 2	Grt 2	Grt 2	Grt 2	Grt 2	Grt 2	Grt 2	Grt 2	Grt 2	Grt 2	Grt 2	Grt 2	
		→	→	→	→	→	→	→	→	→	→	→	→	→	→	→	→	→	Rim	Rim	
SiO ₂		40.49	40.09	40.42	39.74	39.69	39.46	40.38	40.60	40.38	40.76	40.72	40.71	40.85	40.36	40.79	40.69	40.43	40.44	40.33	
TiO ₂		0.02	0.03	0.00	0.01	0.05	0.03	0.00	0.03	0.02	0.06	0.00	0.03	0.02	0.01	0.05	0.02	0.02	0.02	0.00	
Al ₂ O ₃		22.15	21.97	22.26	21.94	21.96	21.80	22.29	22.23	22.66	22.71	22.54	22.57	22.36	22.62	22.29	22.32	22.44	22.49	22.18	
FeO*		20.18	20.59	20.76	22.39	23.67	24.74	20.16	20.28	19.80	19.68	20.57	20.54	20.72	19.99	20.73	21.43	20.74	20.62	21.40	
MnO		0.43	0.52	0.53	0.74	1.05	1.60	0.53	0.52	0.37	0.39	0.36	0.52	0.47	0.49	0.48	0.42	0.47	0.39	0.57	
MgO		7.00	7.02	6.48	5.11	4.21	3.73	7.06	7.10	7.68	8.08	7.72	7.32	7.23	7.09	7.03	7.08	7.08	6.84	6.44	
CaO		9.32	9.48	9.30	9.24	8.94	8.82	10.03	9.82	9.37	9.11	8.95	9.23	9.19	9.26	9.03	9.24	9.49			
Total		99.59	99.70	99.75	99.17	99.57	100.18	100.45	100.58	100.28	100.79	100.86	100.64	100.88	99.75	100.63	100.99	100.42	100.51	100.41	
<i>Cations on the basis of 12 oxygens</i>																					
Si		3.11	3.07	3.11	3.10	3.11	3.09	3.07	3.08	3.06	3.07	3.08	3.09	3.09	3.10	3.09	3.08	3.08	3.08	3.08	
Ti		0.00	0.00	0.00	0.00	0.00	0.00	0.00	0.00	0.00	0.00	0.00	0.00	0.00	0.00	0.00	0.00	0.00	0.00	0.00	
Al		2.00	1.99	2.02	2.02	2.03	2.01	2.00	1.99	2.03	2.02	2.01	2.02	2.00	2.04	2.00	2.02	2.01	2.02	2.00	
Fe ³⁺		0.00	0.00	0.00	0.00	0.00	0.00	0.00	0.00	0.00	0.00	0.00	0.00	0.00	0.00	0.00	0.00	0.00	0.00	0.00	
Fe ²⁺		1.29	1.32	1.33	1.46	1.55	1.62	1.28	1.29	1.26	1.24	1.30	1.31	1.31	1.28	1.32	1.36	1.32	1.31	1.37	
Mn		0.03	0.04	0.03	0.05	0.07	0.10	0.03	0.03	0.02	0.02	0.03	0.03	0.03	0.03	0.03	0.03	0.03	0.03	0.04	
Mg		0.80	0.80	0.74	0.60	0.49	0.44	0.80	0.81	0.87	0.91	0.87	0.83	0.82	0.81	0.80	0.80	0.77	0.73	0.73	
Ca		0.77	0.78	0.77	0.75	0.74	0.82	0.80	0.76	0.74	0.72	0.73	0.75	0.75	0.73	0.75	0.75	0.79	0.78		
Total		8.00	8.00	8.00	8.00	8.00	8.00	8.00	8.00	8.00	8.00	8.00	8.00	8.00	8.00	8.00	8.00	8.00	8.00	8.00	
X _{Pp}		0.28	0.27	0.26	0.21	0.17	0.15	0.27	0.28	0.30	0.31	0.30	0.29	0.28	0.28	0.27	0.27	0.28	0.27	0.25	
X _{alm}		0.45	0.45	0.46	0.51	0.54	0.56	0.44	0.43	0.43	0.44	0.45	0.45	0.45	0.46	0.46	0.47	0.45	0.45	0.47	
X _{Grs}		0.26	0.27	0.27	0.26	0.25	0.28	0.27	0.26	0.25	0.25	0.26	0.25	0.26	0.26	0.25	0.26	0.27	0.27	0.27	
X _{Sps}		0.01	0.01	0.01	0.03	0.04	0.01	0.01	0.01	0.01	0.01	0.01	0.01	0.01	0.01	0.01	0.01	0.01	0.01	0.01	

Sample		ES 21-2		
--------	--	---------	--	--

Table 1. (continued)

Sample	ES 21-2																		ES 20-1							
	73	74	75	76	77	78	79	1	2	3	4	5	6	7	8	9	91	92	93							
Analysis	Grt 1	Grt 1	Grt 1	Grt 1	Grt 1	Grt 1	Grt 1	Grt 1	Grt 1	Grt 1	Grt 1	Grt 1	Grt 1	Grt 1	Grt 1	Grt 1	Grt 2	Grt 2	Grt 2	Rim	→	→	→	→	→	
Mode																	Mantle									
SiO ₂	38.24	38.83	38.31	38.26	38.63	38.75	38.77	37.92	38.14	38.09	38.14	38.52	38.35	38.47	37.48	38.50	39.72	39.07	39.39							
TiO ₂	0.04	0.26	0.21	0.09	0.08	0.16	0.12	0.11	0.00	0.00	0.11	0.10	0.00	0.16	0.00	0.06	0.10	0.14	0.12							
Al ₂ O ₃	20.83	20.57	21.04	21.21	21.01	21.13	21.41	21.81	21.88	22.32	21.55	21.54	21.20	21.29	20.93	20.77	21.18	21.48	21.22							
FeO*	23.69	22.86	23.52	23.56	23.87	23.70	22.95	21.73	21.31	22.62	21.88	23.82	24.65	23.83	26.38	25.37	21.77	21.65	21.68							
MnO	1.01	0.98	1.34	1.43	1.43	1.34	1.24	0.36	0.69	0.76	0.68	1.04	0.77	0.65	1.42	1.75	0.54	0.52	0.51							
MgO	5.06	5.44	5.34	5.30	5.38	5.23	5.41	6.25	6.18	6.49	6.38	4.26	4.32	4.60	3.33	3.45	7.01	6.85	6.79							
CaO	10.31	10.04	10.11	10.40	10.28	10.46	10.03	10.82	11.14	11.06	10.59	11.21	11.32	10.37	11.21	9.99	10.40	10.78	10.61							
Total	99.18	98.98	99.87	100.25	100.68	100.77	99.93	99.00	99.34	101.34	99.33	100.49	100.61	99.37	100.75	99.88	100.72	100.49	100.32							
<i>Cations on the basis of 12 oxygens</i>																										
Si	3.00	3.04	2.98	2.96	2.98	2.99	3.01	2.94	2.95	2.89	2.95	2.99	2.97	3.01	2.93	3.03	3.02	2.98	3.02							
Ti	0.00	0.02	0.01	0.01	0.01	0.01	0.01	0.01	0.00	0.00	0.00	0.00	0.00	0.01	0.00	0.00	0.00	0.00	0.01							
Al	1.92	1.90	1.93	1.94	1.91	1.92	1.96	2.00	1.99	1.99	1.97	1.97	1.94	1.97	1.93	1.90	1.93	1.93	1.91							
Fe ³⁺	0.08	0.00	0.09	0.13	0.12	0.08	0.01	0.11	0.11	0.23	0.12	0.05	0.12	0.00	0.21	0.00	0.04	0.09	0.04							
Fe ²⁺	1.47	1.50	1.44	1.40	1.42	1.45	1.47	1.30	1.27	1.21	1.30	1.50	1.48	1.56	1.51	1.67	1.35	1.30	1.34							
Mn	0.07	0.06	0.09	0.09	0.09	0.08	0.02	0.05	0.05	0.04	0.07	0.05	0.04	0.04	0.09	0.12	0.04	0.03	0.03							
Mg	0.59	0.64	0.62	0.61	0.62	0.60	0.63	0.72	0.71	0.73	0.74	0.49	0.50	0.54	0.41	0.80	0.78	0.78	0.78							
Ca	0.87	0.84	0.84	0.86	0.85	0.86	0.83	0.90	0.92	0.90	0.88	0.93	0.94	0.87	0.94	0.84	0.85	0.88	0.87							
Total	8.00	8.00	8.00	8.00	8.00	8.00	8.00	8.00	8.00	8.00	8.00	8.00	8.00	8.00	8.00	8.00	8.00	8.00	8.00							
X _{Prp}	0.20	0.21	0.21	0.21	0.21	0.20	0.21	0.25	0.25	0.25	0.17	0.17	0.18	0.13	0.13	0.26	0.26	0.26	0.26							
X _{alm}	0.49	0.49	0.48	0.47	0.48	0.48	0.49	0.44	0.43	0.42	0.44	0.50	0.50	0.52	0.52	0.55	0.45	0.43	0.44							
X _{Grs}	0.29	0.28	0.28	0.29	0.28	0.29	0.28	0.30	0.31	0.31	0.30	0.31	0.32	0.29	0.32	0.28	0.28	0.30	0.29							
X _{Sps}	0.02	0.02	0.03	0.03	0.03	0.03	0.02	0.01	0.02	0.02	0.01	0.02	0.01	0.01	0.01	0.04	0.04	0.01	0.01							

*Total Fe as FeO

Sample	ES 20-1																								
	94	95	96	97	98	99	100	101	102	103	104	105	106	107	108	109	110	91	91						
Analysis	Grt 2	Grt 2	Grt 2	Grt 2	Grt 2	Grt 2	Grt 2	Grt 2	Grt 2	Grt 2	Grt 2	Grt 2	Grt 2	Grt 2	Grt 2	Grt 2	Grt 2	Grt 2	Grt 2	Rim	→	→	→	→	→
Mode																									
SiO ₂	39.62	39.48	39.26	39.09	38.07	38.84	38.29	39.07	39.27	38.97	38.60	38.88	39.38	39.17	38.76	38.99	38.98	40.60	40.57						
TiO ₂	0.06	0.05	0.01	0.03	0.04	0.07	0.02	0.04	0.05	0.06	0.01	0.09	0.08	0.12	0.06	0.03	0.00								
Al ₂ O ₃	21.72	21.74	21.57	21.94	21.71	21.84	21.59	21.60	21.68	21.52	21.57	21.54	21.37	21.56	21.25	21.30	21.36	22.19	22.58						
FeO*	21.78	21.73	21.92	21.70	21.63	21.84	22.09	21.75	21.77	21.61	22.67	21.34	21.40	21.66	21.29	21.15	20.89	20.93	20.69						
MnO	0.53	0.57	0.55	0.53	0.57	0.57	0.56	0.54	0.53	0.54	0.51	0.51	0.49	0.42	0.45	0.42	0.42	0.38	0.42						
MgO	7.02	7.05	7.12	7.19	7.19	6.95	6.74	7.00	7.08	7.12	6.31	6.36	6.44	6.52	6.63	6.68	7.18	7.59							
CaO	10.08	9.96	10.01	10.16	10.09	10.64	10.35	10.42	10.49	10.34	11.14	11.29	11.44	11.50	11.51	11.50	11.50	9.24	9.12						
Total	100.81	100.58	100.44	100.64	99.29	100.72	99.69	100.40	100.86	100.15	100.86	99.93	100.60	100.84	99.86	100.11	99.89	100.55	100.97						
<i>Cations on the basis of 12 oxygens</i>																									
Si	3.01	3.01	3.00	2.98	2.94	2.95	2.95	2.98	2.98	2.98	2.95	2.99	3.01	2.98	2.98	2.99	2.99	3.09	3.06						
Ti	0.00	0.00	0.00	0.00	0.00	0.00	0.01	0.00	0.00	0.00	0.00	0.00	0.01	0.00	0.00	0.00	0.01	0.00	0.00						
Al	1.95	1.95	1.94	1.97	1.97	1.96	1.96	1.94	1.94	1.94	1.95	1.95	1.92	1.94	1.92	1.93	1.99	2.01							
Fe ³⁺	0.02	0.03	0.06	0.08	0.15	0.13	0.13	0.09	0.09	0.09	0.16	0.07	0.05	0.09	0.11	0.09	0.00	0.00	0.00						
Fe ²⁺	1.37	1.36	1.33	1.30	1.24	1.26	1.29	1.30	1.30	1.29	1.29	1.30	1.31	1.29	1.26	1.26	1.26	1.33	1.31						
Mn	0.03	0.04	0.04	0.03	0.04	0.04	0.04	0.04	0.04	0.03	0.03	0.03	0.03	0.03	0.03	0.03	0.03	0.03	0.03						
Mg	0.80	0.80	0.81	0.81	0.83	0.79	0.77	0.80	0.80	0.81	0.72	0.73	0.73	0.73	0.75	0.76	0.76	0.82	0.85						
Ca	0.82	0.81	0.82	0.83	0.83	0.87	0.85	0.85	0.85	0.85	0.91	0.93	0.94	0.94	0.95	0.95	0.95	0.75	0.74						
Total	8.00	8.00	8.00	8.00	8.00	8.00	8.00	8.00	8.00	8.00	8.00	8.00	8.00	8.00	8.00	8.00	8.00	8.00	8.00						
X _{Prp}	0.27	0.27	0.27	0.27	0.28	0.27	0.26	0.27	0.27	0.24	0.25	0.24	0.25	0.25	0.25	0.25	0.25	0.25	0.25						
X _{alm}	0.45	0.45	0.45	0.44	0.42	0.43	0.4																		